Published for SISSA by Springer

Received: January 7, 2021
Revised: February 14, 2021
Accepted: February 23, 2021
Published: March 30, 2021

Rise of the DIS structure function F_L at small x caused by double-logarithmic corrections

B.I. Ermolaev[a,1] **and S.I. Troyan**[b]

[a] *Ioffe Physico-Technical Institute, 194021 St. Petersburg, Russia*
[b] *St.Petersburg Institute of Nuclear Physics NRC KI, 188300 Gatchina, Russia*

E-mail: boris.ermolaev@cern.ch, sergei.troyan@thd.pnpi.spb.ru

Abstract: We present calculation of F_L in the double-logarithmic approximation (DLA) and demonstrate that the synergic effect of the factor $1/x$ from the α_s^2-order and the steep x-dependence of the totally resummed double logarithmic contributions of higher orders ensures the power-like rise of F_L at small x and arbitrary Q^2.

Keywords: Deep Inelastic Scattering (Phenomenology)

ArXiv ePrint: 2012.10633

[1] Corresponding author.

https://doi.org/10.1007/JHEP03(2021)274

Contents

1 Introduction

Theoretical investigation of the DIS structure function $F_L(x, Q^2)$ (and other DIS structure functions) in the context of perturbative QCD began with calculations in the fixed orders in α_s. First, there were calculations in the Born approximation, then more involved first-loop and second-loop calculations (see refs. [1–19]) followed by the third-order results(see ref. [20]). All fixed-order calculations showed that F_L decreases at small x. Alternative approach to study F_L was applying all-order resummations. In the first place, F_L was studied with DGLAP(see refs. [21–24]) and its NLO modifications. In addition, there are approaches where DGLAP is combined with BFKL(see refs. [25–29]), see e.g. refs. [30, 31]. Besides, there are calculations in the literature based on the dipole model, see refs. [34, 35]. This approach was used in the global analysis of experimental data in ref. [36]. Let us notice that ref. [37] contains detailed bibliography on this issue.

Applying DGLAP to studying F_L is model-independent. However according to ref. [37], neither LO DGLAP nor the NLO DGLAP modifications ensure the needed rise of F_L at small x and disagree with experimental data at small Q^2, which sounds quite natural because DGLAP by definition is not supposed to be used in the region of small Q^2. The modifications of DGLAP in refs. [30, 31] are based on treating BFKL as a small-x input for the DGLAP equations. The approach of ref. [32] treats the Pomeron intercept as a parameter fixed from experiment.

In this paper we present an alternative approach to calculate F_L: total resummation of double-logarithmic (DL) contributions to F_L, accounting for both logarithms of x and Q^2. The method we use is self-consistent and does not involve any models. We modify the approach which we used in ref. [38] to calculate F_1 in the Double-Logarithmic Approximation (DLA). This approach has nothing in common with the BFKL equation and its ensuing modifications. Indeed, instead of summing leading logarithms, i.e. the contributions $\sim (1/x)\,(\alpha_s \ln(1/x))$, we sum the DL contributions $\sim \alpha_s \ln^2(1/x)$ as well as the DL of Q^2. Because of the absence of the factor $1/x$ such contributions were commonly neglected by the HEP community for a long time. However, it has recently been proved in ref. [38] that the DL contribution to Pomeron is not less important than the BFKL contribution.

We calculate F_L in DLA with constructing and solving Infra-Red Evolution Equations (IREEs). As is well-known, the IREE approach was suggested by L.N. Lipatov in refs, [39–42]. It proved to be a simple and efficient instrument (see e.g. the overviews in refs. [43, 44]) for calculating many objects in QCD and Standard Model. Constructing and solving IREEs, we obtain general solutions. In order to specify them one has to define the starting point (input) for IREEs. Conventionally in the IREE technology the Born contributions have been chosen as the inputs. However, $F_L = 0$ in the Born approximation, so the input has to be chosen anew. We suggest that the second-loop expression for F_L can play the role of the input and arrive thereby to explicit expressions for perturbative components of F_L. We demonstrate that the total resummation of DL contributions together with the factor $1/x$ appearing in the α_s^2-order provide F_L with the rise at small x.

We start with considering F_L in the large-Q^2 kinematic region

$$Q^2 > \mu^2, \tag{1.1}$$

with μ being a mass scale. Then we present a generalization of our results to small Q^2. The scale μ is often associated with the factorization scale. The value of μ is arbitrary[1] except the requirement $\mu > \Lambda_{QCD}$ to guarantee applicability of perturbative QCD.

Our paper is organized as follows: in section 2 we introduce definitions and notations, then remind how to calculate F_L through auxiliary invariant functions. Calculations of F_L in the α_s^2-order are considered in section 3. We represent them in the way convenient for analysis of contributions from higher loops. Then we explain how to realize our strategy: combining the non-logarithmic results from the α_s^2-order with double-logarithmic (DL) contributions from higher-order graphs. Total resummation of DL contributions to F_L is done in section 4 through constructing and solving IREEs. IREEs control both x and Q^2

[1] For specifying μ on basis of Principle of Minimal Sensitivity (defined in ref. [45]) see refs. [43, 44].

JHEP03(2021)274

-evolutions of F_L from the starting point. Specifying the input is done in section 5. In section 6 we present explicit expressions for leading small-x contributions to perturbative components of F_L. To make clearly seen the rise of F_L at small x we present the small-x asymptotics of F_L. After that we compare our results for F_L at small-x with the ones predicted by approaches involving BFKL. Then we consider the generalization of our results on F_L in region defined by eq. (1.1) to the small-Q^2 region. Finally, section 7 is for concluding remarks.

2 Calculating F_L through auxiliary amplitudes

The most convenient way to calculate $F_{1,2}$ and F_L in Perturbative QCD is the use of auxiliary invariant amplitudes. Below we remind how this approach works. The unpolarized part of the hadronic tensor describing the lepton-hadron DIS is

$$W_{\mu\nu}(p,q) = \left(-g_{\mu\nu} + \frac{q_\mu q_\nu}{q^2}\right) F_1 + \frac{1}{pq}\left(p_\mu - q_\mu \frac{pq}{q^2}\right)\left(p_\nu - q_\nu \frac{pq}{q^2}\right) F_2 \tag{2.1}$$

and each of F_1, F_2 depends on Q^2 and $x = Q^2/w$, with $Q^2 = -q^2$ and $w = 2pq$.

$$-A \equiv g_{\mu\nu} W_{\mu\nu} = 3F_1 + \frac{F_2}{2x} + O(p^2), \tag{2.2}$$

$$B \equiv \frac{p_\mu p_\nu}{pq} W_{\mu\nu} = -\frac{1}{2x} F_1 + \frac{1}{4x^2} F_2 + O(p^2), \tag{2.3}$$

where we use the standard notatons $x = -q^2/w = Q^2/w$, $w = 2pq$. Neglecting terms $\sim p^2$, we express $F_{1,2}$ through A and B:

$$\begin{aligned} F_1 &= \frac{A}{2} + xB, \\ F_2 &= 2xF_1 + 4x^2 B, \end{aligned} \tag{2.4}$$

so that

$$F_L = F_2 - 2xF_1 = 4x^2 B. \tag{2.5}$$

Each of F_1, F_2 includes both perturbative and non-perturbative contributions. According to the QCD factorization concept, these contributions can be separated. In scenario of the single-parton scattering, F_1, F_2 can be represented in any available form of QCD factorization through the following convolutions (see figure 1):

$$F_1 = F_1^{(q)} \otimes \Phi_{(q)} + F_1^{(g)} \otimes \Phi_{(g)}, \qquad F_2 = F_2^{(q)} \otimes \Phi_{(q)} + F_2^{(g)} \otimes \Phi_{(g)}, \tag{2.6}$$

where $\Phi_{1,2}^{(q,g)}$ stand for initial parton distributions whereas $F_1^{(q,g)}, F_2^{(q,g)}$ are perturbative components of the structure functions F and F_2 respectively. The superscripts $q(g)$ in Eq, (2.6) mean that the initial partons in the perturbative Compton scattering are quarks (gluons). The DIS off the partons is parameterized by the same way as eq. (2.1):

$$W_{\mu\nu}^{(q,g)}(p,q) = \left(-g_{\mu\nu} + \frac{q_\mu q_\nu}{q^2}\right) F_1^{(q,g)} + \frac{1}{pq}\left(p_\mu - q_\mu \frac{pq}{q^2}\right)\left(p_\nu - q_\nu \frac{pq}{q^2}\right) F_2^{(q,g)}, \tag{2.7}$$

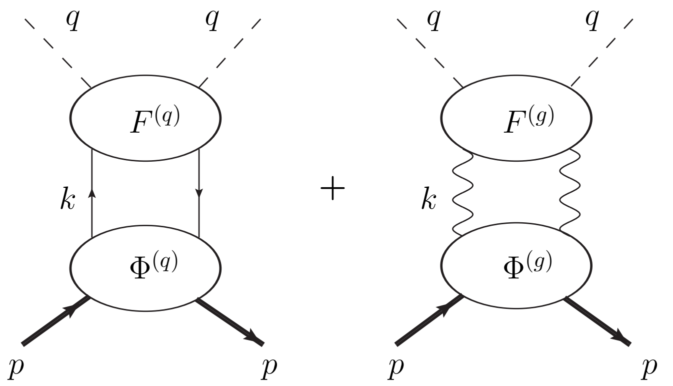

Figure 1. QCD factorization for DIS structure functions. Dashed lines denote virtual photons. The upper blobs describe DIS off partons. The straight (waved) vertical lines denote virtual quarks (gluons). The lowest blobs correspond to initial parton distributions in the hadrons. $F^{(q,g)}$ is a generic notation for perturbative components of $F_1^{(q,g)}$, $F_2^{(q,g)}$ and $F_L^{(q,g)}$.

with p denoting the initial parton momentum. Throughout the paper we will neglect virtualities p^2, presuming the initial partons to be nearly on-shell. Introducing the auxiliary amplitudes $A^{(q,g)}$ and $B^{(q,g)}$ similarly to eqs. (2.2), (2.3), one can express $F_1^{(q,g)}$ and $F_2^{(q,g)}$ in terms of $A^{(q,g)}$ and $B^{(q,g)}$ so that

$$F_L^{(q,g)} = F_2^{(q,g)} - 2xF_1^{(q,g)} = 4x^2 B^{(q,g)}, \tag{2.8}$$

with

$$B^{(q,g)} = \frac{p_\mu p_\nu}{pq} W_{\mu\nu}^{(q,g)}. \tag{2.9}$$

Applying (2.8), (2.9) to $W_{\mu\nu}^{(q,g)}$ in the Born and the first-loop approximation yields (see refs. [1]–[19]) that $F_L^{(q)} = F_L^{(g)} = 0$ in the Born approximation whereas the first-loop results are:

$$\left(F_L^{(q)}\right)_{(1)} = \frac{2\alpha_s}{\pi} C_F x^2, \quad \left(F_L^{(g)}\right)_{(1)} = \frac{4\alpha_s}{\pi} n_f x^2 (1-x). \tag{2.10}$$

Eq. (2.10) suggests that F_L should decrease $\sim x^2$ at $x \to 0$. However, the second-loop results exhibit a slower decrease.

3 Leading contributions to B in the second-loop approximation

The second loop brings a radical change to the small-x behaviour of B compared to the first-loop result. Namely, there appear contributions $\sim 1/x$ in contrast to logarithmic dependence of B in the first loop. Such contributions were calculated in ref. [14]. Nevertheless, we prefer to repeat these calculations in order to represent the results in the way convenient for applying to the total resummation of higher loops in DLA.

In the first place we consider ladder graphs contributing to B, The ladder graphs contributing to $W_{\mu\nu}$ in the α_s^2-order are depicted in figure 2. Graphs (a) and (b) correspond to DIS off quarks whereas graphs (c) and (d) are for DIS off gluons. Calculations in the

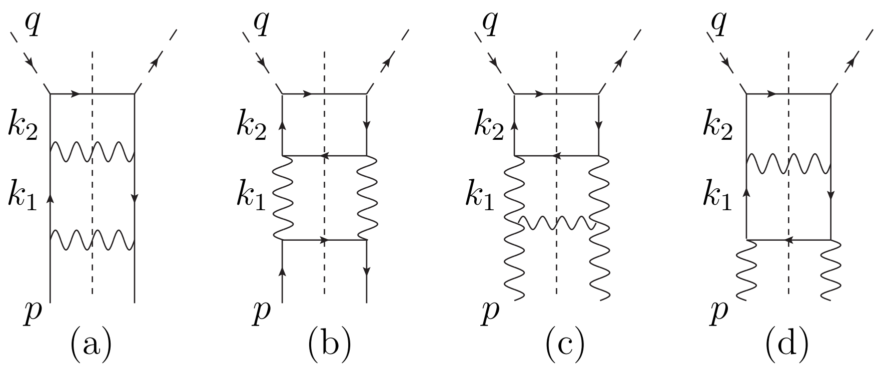

Figure 2. Ladder graphs for $F_1^{(q,g)}$, $F_2^{(q,g)}$ and $F_L^{(q,g)}$ in the second-loop approximation. Graphs (a) and (b) correspond to DIS off quarks and graphs (c) and (d) are for DIS off gluons.

small-x kinematics are simpler when the Sudakov variables (see ref. [46]) are used. In terms of them, momenta k_i of virtual partons are parameterized as follows:

$$k_i = \alpha_i q' + \beta_i p' + k_{i\perp}, \tag{3.1}$$

where q' and p' are the massless (light-cone) momenta made of momenta p and q:

$$p' = p - q(p^2/w) \approx p, \quad q' = q - p(q^2/w) = q + xp. \tag{3.2}$$

In eq. (3.2) q denotes the virtual photon momentum while p is momentum of the initial parton. We remind that we presume that p^2 is small, so we will neglect it throughout the paper. Invariants involving k_i looks as follows in terms of the Sudakov invariants:

$$\begin{aligned} k_i^2 &= w\alpha_i\beta_i - k_{i\perp}^2 = w(\alpha_i\beta_i - z_i), \quad 2pk_i = w\alpha_i, \quad 2qk_i = w(\beta_i - x\alpha_i), \\ 2k_ik_j &= w(\alpha_i - \alpha_j)(\beta_i - \beta_j) - k_{i\perp}^2 - k_{j\perp}^2 = w\left((\alpha_i - \alpha_j)(\beta_i - \beta_j) - z_i - z_j\right). \end{aligned} \tag{3.3}$$

We have introduced in eq. (3.3) dimensionless variables $z_{i,j}$ defined as follows:

$$z_i = k_{i\perp}^2/w. \tag{3.4}$$

3.1 Contributions to B for DIS off quarks

We start with calculating the second-loop contribution $B_q^{(a)}$ of the two-loop ladder graph (a) in figure 2 to B for DIS off quarks. It is given by the following expression:

$$B^{(2a)} = C_q^{(2b)} \chi_2 w \int d\alpha_{1,2} d\beta_{1,2} dk_{1,2\perp}^2 \frac{N^{(2a)}}{k_1^2 k_1^2 k_2^2 k_2^2} \delta\left((q+k_2)^2\right) \delta\left((k_1-k_2)^2\right) \delta\left((p-k_1)^2\right), \tag{3.5}$$

where $C_q^{(2b)} = C_F^2$,

$$\chi_2 = \frac{\alpha_s^2}{8\pi} \tag{3.6}$$

and

$$N^{(2a)} = \frac{1}{2}\mathrm{Tr}\left[\hat{p}\gamma_{\lambda_1}\hat{k}_1\gamma_{\lambda_2}\hat{k}_2\hat{p}(\hat{q}+\hat{k}_2)\hat{p}\hat{k}_2\gamma_{\lambda_2}\hat{k}_1\gamma_{\lambda_1}\right] \tag{3.7}$$
$$= 2k_1^2\mathrm{Tr}\left[\hat{k}_2(\hat{k}_1-\hat{p})\hat{k}_2\hat{p}(\hat{q}+\hat{k}_2)\hat{p}\right]$$
$$= 2k_1^2(w+2pk_2)\mathrm{Tr}\left[\hat{k}_2(\hat{k}_1-\hat{p})\hat{k}_2\hat{p}\right].$$

We represent it as the sum of $N_1^{(2a)}$ and $N_2^{(2a)}$:

$$N^{(2a)} = N_1^{(2a)} + N_2^{(2a)} \tag{3.8}$$

with

$$N_1^{(2a)} = -4k_1^2\left((2pk_2)^3 + w(2pk_2)^2\right) \tag{3.9}$$

and

$$N_2^{(2a)} = 4k_1^2\left[\left(k_1^2+k_2^2\right)\left((2pk_2)^2 + w(2pk_2)\right) - k_1^2k_2^2(2pk_2) - wk_1^2k_2^2\right], \tag{3.10}$$

In eqs. (3.9), (3.10) we have used the quark density matrix

$$\hat{\rho}(p) = \frac{1}{2}\hat{p} \tag{3.11}$$

and made use of the δ-functions of eq. (3.5). They yield that $2k_1k_2 = k_1^2 + k_2^2$ and $2pk_1 = k_1^2$. It turns out that the leading contributions comes from N_1^{2a}, so first of all we consider it. Throughout the paper we will use dimensionless variables $z_{1,2}$ instead of $k_{1,2\perp}^2$:

$$z_1 = k_{1\perp}^2/w\,, \qquad z_2 = k_{2\perp}^2/w\,, \qquad z = z_1 + z_2. \tag{3.12}$$

It is also convenient to use the variable l defined as follows:

$$l = \beta_1 - \beta_2. \tag{3.13}$$

Using the δ-functions to integrate (3.5) over $\alpha_{1,2}$ and β_2 and replacing $N^{(2a)}$ by $N_1^{(2a)}$ we are left with three more integrations:

$$B^{(2a)} \approx 4C_F^2\chi_2\int_\lambda^1\frac{dz_1}{z_1}\int_\lambda^1\frac{dz_2}{z_2^2}\int_z^1 dl\left[-\frac{z^3}{l^2(l+\eta)^2} + \frac{z^2}{l(l+\eta)^2}\right], \tag{3.14}$$

with η defined as follows:

$$\eta = \frac{z(x+z_2)}{z_2}. \tag{3.15}$$

Details of calculation in eq. (3.14) can be found in appendix A. Let us remind that throughout this paper we focus on the small-x region. The most important contributions in eq. (3.14) at small x are $\sim 1/x$. Retaining them only and integrating (3.14) with logarithmic accuracy, we arrive at

$$B^{(2a)} \approx C_q^{(2a)}\gamma^{(2)}\,x^{-1}, \tag{3.16}$$

JHEP03(2021)274

with

$$\gamma^{(2)} = 4\chi_2 \rho \ln 2, \tag{3.17}$$

where χ_2 is defined in (3.6) and

$$\rho = \ln(w/\mu^2), \tag{3.18}$$

with μ being an infrared cut-off. Contribution to B of graph (b) in figure 2 is given by the following expression:

$$B^{(2b)} = C_q^{(2b)} \chi_2 w \int d\alpha_{1,2} d\beta_{1,2} dk_{1,2\perp}^2 \frac{N^{(2b)}}{k_1^2 k_1^2 k_2^2 k_2^2} \delta\left((q+k_2)^2\right) \delta\left((k_1-k_2)^2\right) \delta\left((p-k_1)^2\right), \tag{3.19}$$

where $C_q^{(2b)} = n_f C_F$ and

$$N^{(2b)} = p_\mu p_\nu \mathrm{Tr}\left[\gamma_\nu \left(\hat{q}+\hat{k}_2\right) \gamma_\mu \hat{k}_2 \gamma_{\lambda'} \left(\hat{k}_1 - \hat{k}_2\right) \gamma_{\sigma'} \hat{k}_2\right] \left(p_{\lambda'} k_{1\sigma'} + k_{1\lambda'} p_{1\sigma'}\right) . \tag{3.20}$$

Apart from the color factor $C_F/2$, the integrand in eq. (3.19) coincides with the integrand of eq. (3.5), so we obtain the same leading contribution:

$$B^{(2b)} \approx C_q^{(2b)}\ x^{-1} \gamma^{(2)}, \tag{3.21}$$

where $\gamma^{(2)}$ is given by eq. (3.17) and $C_q^{(2b)} = C_F/2$. Our analysis of non-ladder graphs shows that they do not bring the factor $1/x$ because they do not contain $(k_2^2)^2$ in denominators. Therefore, the total leading contribution $B_q^{(2)}$ to B_q in the second loop is

$$B_q^{(2)} = \left(C_q^{(2a)} + C_q^{(2b)}\right) \gamma^{(2)}\ x^{-1} \equiv C_q^{(2)} \gamma^{(2)}\ x^{-1}. \tag{3.22}$$

Now let us consider some important technical details concerning eqs. (3.16) (the same reasoning holds for eq. (3.21)). This result stems from the terms in eq. (3.7) where momenta k_2 are coupled with the external momenta p and q. The other terms in eq. (3.7) (i.e. the ones $\sim k_2^2, k_1 k_2$) either cancel k_2^2 in the denominator of eq. (3.5), preventing appearance of the factor $1/x$, or cancel $1/k_1^2$, killing $\ln w$. Hence, the first step to calculate the trace in eq. (3.7) can be reducing the trace down to $\mathrm{Tr}[\hat{p}\hat{k}_2\hat{p}\hat{k}_2]$. Obviously, it corresponds to neglecting the factor $2pk_1$ in $\hat{k}_1\hat{p}\hat{k}_1$:

$$\hat{k}_1 \hat{p} \hat{k}_1 = 2pk_1 \hat{k}_1 - k_1^2 \hat{p} \approx -k_1^2 \hat{p} . \tag{3.23}$$

This observation allows us to develop a strategy to select most important contributions to B in arbitrary orders in α_s. In other words, the non-singlet component of F_L can be calculated in DLA in the straightforward way, without evolution equations.

3.2 Contributions to B for DIS off gluons

The second-loop contributions to the DIS off the initial gluon correspond to the ladder graphs (c,d) in figure 2. We calculate their joint contribution B_g to F_L. Obviously, the contribution of graph (c) is

$$B^{(2c)} = C_g^{(2)} \chi^{(2)} \int dz_{1,2} d\beta_{1,2} d\alpha_{1,2} \frac{N^{(2c)}}{k_1^2 k_1^2 k_2^2 k_2^2} \delta\left((p-k_1)^2\right) \delta\left((k_1-k_2)^2\right) \delta\left((q+k_2)^2\right), \tag{3.24}$$

where $\chi^{(2)}$ is defined in eq. (3.6) and $C_g^{(2)} = n_f N$. The numerator $N^{(2c)}$ is defined as follows:

$$N^{(2c)} = p_\mu p_\nu \mathrm{Tr}\left[\gamma_\nu \left(\hat{q} + \hat{k}_2\right) \gamma_\mu \hat{k}_2 \gamma_{\lambda'} \left(\hat{k}_1 - \hat{k}_2\right) \gamma_{\sigma'} \hat{k}_2\right] H_{\lambda'\sigma'} \,, \tag{3.25}$$

with

$$H_{\lambda'\sigma'} = H_{\lambda'\sigma'\lambda\sigma} \rho_{\lambda\sigma} \ . \tag{3.26}$$

In eq. (3.26) the notation $H_{\lambda'\sigma'\lambda\sigma}$ stands for the ladder gluon rung while $\rho_{\lambda\sigma}$ denotes the gluon density matrix for the initial gluons which we treat as slightly virtual:

$$\begin{aligned} H_{\lambda'\sigma'\lambda\sigma} = &- \left[(2k_1 - p)_\lambda g_{\lambda'\tau} + (2p - k_1)_{\lambda'} g_{\lambda\tau} + (-k_1 - p)_\tau g_{\lambda'\lambda}\right] \\ &\left[(2k_1 - p)_\sigma g_{\sigma'\tau} + (2p - k_1)_{\sigma'} g_{\sigma\tau} + (-k_1 - p)_\tau g_{\beta\sigma}\right] \ . \end{aligned} \tag{3.27}$$

The terms $\sim p_\lambda, p_\sigma$ in eq. (3.27) can be dropped because of the gauge invariance. We use the Feynman gauge for the initial gluons:

$$\rho_{\lambda\sigma} = -\frac{1}{2} g_{\lambda\sigma} \ . \tag{3.28}$$

As a result we obtain

$$H_{\lambda'\sigma'} = 8 p_{\lambda'} p_{\sigma'} - 4(p_{\lambda'} k_{1\sigma'} + k_{1\lambda'} p_{\sigma'}) + 2 k_{1\lambda'} k_{1\sigma'} + 3 g_{\lambda'\sigma'} k_1^2. \tag{3.29}$$

We have used in the last term of eq. (3.29) that $2pk_1 \approx k_1^2$. DL contributions to the gluon ladder come from the kinematics where $\lambda' \in R_L, \sigma' \in R_T$ or vice versa (the symbols R_L and R_T denote the longitudinal and transverse momentum spaces respectively). Therefore, the leading term in eq. (3.27) in DLA is

$$H^{DL}_{\lambda'\sigma'} = -4 \left(p_{\lambda'} k_{1\sigma'} + k_{1\lambda'} p_{\sigma'}\right) \tag{3.30}$$

while $2k_{1\lambda'} k_{1\sigma'}$ brings corrections to it. The first term in eq. (3.29) contain the longitudinal momenta only and the last term vanishes at $\lambda' \neq \sigma'$. Substituting eq. (3.30) in eq. (3.25) we obtain

$$\begin{aligned} N^{(2c)} \; = \; & \mathrm{Tr}\left[\hat{p}\left(\hat{q} + \hat{k}_2\right) \hat{p}\hat{k}_2\hat{p}\left(\hat{k}_1 - \hat{k}_2\right) \hat{k}_{1\perp}\hat{k}_2\right] + \mathrm{Tr}\left[\hat{p}\left(\hat{q} + \hat{k}_2\right) \hat{p}\hat{k}_2\hat{k}_{1\perp}\left(\hat{k}_1 - \hat{k}_2\right) \hat{p}\hat{k}_2\right] \\ \approx \; & \mathrm{Tr}\left[\hat{p}\hat{q}\hat{p}\hat{k}_2\hat{p}\left(\hat{k}_1 - \hat{k}_2\right) \hat{k}_{1\perp}\hat{k}_2\right] + \mathrm{Tr}\left[\hat{p}\hat{q}\hat{p}\hat{k}_2\hat{k}_{1\perp}\left(\hat{k}_1 - \hat{k}_2\right) \hat{p}\hat{k}_2\right] \\ = \; & w \mathrm{Tr}\left[\hat{p}\hat{k}_2\hat{p}\left(\hat{k}_1 - \hat{k}_2\right) \hat{k}_{1\perp}\hat{k}_2\right] + w \mathrm{Tr}\left[\hat{p}\hat{k}_2\hat{k}_{1\perp}\left(\hat{k}_1 - \hat{k}_2\right) \hat{p}\hat{k}_2\right] \\ = \; & w 2pk_2 \mathrm{Tr}\left[\hat{p}\left(\hat{k}_1 - \hat{k}_2\right) \hat{k}_{1\perp}\hat{k}_2\right] + w 2pk_2 \mathrm{Tr}\left[\hat{p}\hat{k}_2\hat{k}_{1\perp}\left(\hat{k}_1 - \hat{k}_2\right)\right] \end{aligned} \tag{3.31}$$

Retaining in eq. (3.31) the terms $\sim (pk_2)^2$ and $\sim (pk_2)^3$, we obtain the leading contribution to N_g^{DL}:

$$N^{(2c)} \approx 4(w + 2pk_2)(2pk_2)^2 k_{1\perp}^2 \tag{3.32}$$

which coincides with $N_1^{(2a)}$. Substituting N_g^c in eq. (3.24), representing B_g as

$$B^{(2c)} = C_g^{(2)} \chi^{(2)} I_g \tag{3.33}$$

and then integrating over α_2, we arrive at

$$I_g^{(c)} = \int_\lambda^1 \frac{dz_1}{z_1} \int_\lambda^1 \frac{dz_2}{z_2^2} \int_z^1 dl \left[-\frac{z^3}{l^2(l+\eta)^2} + \frac{z^2}{l(l+\eta)^2} \right] \tag{3.34}$$

with $z, z_{1,2}, l$ and η defined in eqs. (B.2) and (3.15) respectively. The integral in eq. (3.34) coincides with the integral bringing the leading contribution to $B_q^{(2a)}$ in eq. (3.14). obtained for the quark ladder graph and calculated in appendix A. So, we arrive at the leading contribution to B:

$$B^{(2c)} \approx C_g^{(2)} x^{-1} \gamma^{(2)}, \tag{3.35}$$

with $\gamma^{(2)}$ defined in eq. (3.17).

Now we calculate contribution $B^{(2d)}$ to B_g of graph (d) in figure 2. It is given by the following expression:

$$B^{(2d)} = -C_F^2 \chi_2 \int dz_{1,2} d\beta_{1,2} d\alpha_{1,2} \frac{N_g^{(2d)}}{k_1^2 k_1^2 k_2^2 k_2^2} \delta\left((p-k_1)^2\right) \delta\left((k_1-k_2)^2\right) \delta\left((q+k_2)^2\right), \tag{3.36}$$

where χ_2 is defined in eq. (3.6) and $C_g^{(2d)} = n_f C_F$.

$$\begin{aligned} N^{(2d)} &= \frac{1}{2} \mathrm{Tr} \left[\hat{p} \left(\hat{q} + \hat{k}_2 \right) \gamma_\rho \hat{k}_1 \gamma_\lambda \left(\hat{k}_1 - \hat{p} \right) \gamma_\lambda \hat{k}_1 \gamma_\rho \hat{k}_2 \right] \\ &= 2 \left(w + 2pk_2 \right) \mathrm{Tr} \left[\hat{p} \hat{k}_2 \hat{k}_1 \left(\hat{k}_1 - \hat{p} \right) \hat{k}_1 \hat{k}_2 \right], \end{aligned} \tag{3.37}$$

where we have used the gluon density matrix of eq. (3.28). Retaining the terms with pk_2 and neglecting other terms containing k_2, we obtain

$$N^{(2d)} \approx 2 \left(w + 2pk_2 \right) k_1^2 \mathrm{Tr} \left[\hat{p} \hat{k}_2 \hat{p} \hat{k}_2 \right] = 4 \left(w + 2pk_2 \right) (2pk_2)^2 k_1^2 . \tag{3.38}$$

Substituting eq. (3.38) in eq. (3.36), introducing variables $l, z_{1,2}$, then accounting for the δ-functions, we arrive at

$$B^{(2d)} \approx C_g^{(2d)} \chi_2 \int_\lambda^1 \frac{dz_1}{z_1} \int_\lambda^1 \frac{dz_2}{z^2} \int_z^1 \frac{dl}{(l+\eta)^2} \left[-\frac{z^3}{l^2} + \frac{z^2}{l} \right], \tag{3.39}$$

with η defined in eq. (3.15). Comparison of eq. (3.39) with eq. (3.14) shows that the leading contribution, $B_L^{(2d)}$ to B coincides with $B_q^{(2a)}$:

$$B^{(2d)} = C_g^{(2d)} x^{-1} \gamma^{(2)} . \tag{3.40}$$

Therefore, the total leading contribution $B_g^{(2)}$ to B_g in the second loop is

$$B_g^{(2)} = \left(C_g^{(2c)} + C_g^{(2d)} \right) \gamma^{(2)} \ x^{-1} \equiv C_g^{(2)} \gamma^{(2)} \ x^{-1}. \tag{3.41}$$

Eqs. (3.16), (3.21), (3.35) and eq. (3.40) demonstrate explicitly that the only difference between leading contributions of all ladder graphs in figure 2 is different color factors. Combining eqs. (3.22), (3.41) with eq. (2.9) we demonstrate that F_L in the α_s^2-order decreases at $x \to 0$ slower than the first-order result of eq. (2.10). Nevertheless, there are no growth of F_L in the α_s^2-order and in the α_s^3-order as shown in ref. [20]. It suggests that only all-order resummations can provide F_L with some growth.

JHEP03(2021)274

3.3 Remark on the scale of α_s

The factor $\gamma^{(2)}$ defined in eq. (3.17) involves the QCD coupling α_s treated as a constant because of complexity of the two-loop calculations. However, one cannot implement the expressions for $B^{(2)}_{q,g}$ in eqs. (3.22), (3.41) until the scale of α_s has been specified. The adequate parametrization of α_s for processes in the Regge kinematics was obtained in ref. [47] but it cannot be used in $B^{(2)}_{q,g}$ because the leading contributions come the kinematics of virtual partons which is closer to the DGLAP one than to the multi-Regge kinematics. For this reason, we suggest using in $B^{(2)}_{q,g}$ the standard DGLAP parametrization $\alpha_s = \alpha_s(Q^2)$.

3.4 Remark on leading contributions of the ladder graphs in higher loops

Contribution $B^{(n)}_q$ of the quark ladder graph to B in the n^{th} order of the perturbative expansion can be written as follows:

$$\begin{aligned} B^{(n)}_q &= \chi_n C_F^n w^{n-1} \int dk^2_{1\perp} \dots dk^2_{n\perp} d\alpha_1 \dots d\alpha_n d\beta_1 \dots d\beta_n \frac{N^{(n)}_q}{k_1^2 k_1^2 k_2^2 \dots k_n^2} \\ & \delta\left((q+k_n)^2\right) \delta\left((k_n - k_{n-1})^2\right) \dots \delta\left((p-k_1)^2\right), \end{aligned} \tag{3.42}$$

with

$$\chi_n = 2e^2 \left(-\frac{\alpha_s}{2\pi^2}\frac{\pi}{2}\right)^n = 2e^2\left(-\frac{\alpha_s}{4\pi}\right)^n . \tag{3.43}$$

and

$$\begin{aligned} N^{(n)}_q &= \frac{1}{2}\mathrm{Tr}\left[\gamma_{\lambda_1}\hat{k}_1 \dots \gamma_{\lambda_{n-1}}\hat{k}_{n-1}\gamma_{\lambda_{n-1}}\hat{k}_n\gamma_{\lambda_n}\hat{k}_n\hat{p}(\hat{q}+\hat{k}_n)\hat{p}\hat{k}_n\gamma_{\lambda_n}\hat{k}_{n-1}\gamma_{\lambda_{n-1}} \dots \hat{k}_1\gamma_{\lambda_1}\hat{p}\right] \\ &= -(w+2pk_n)\mathrm{Tr}\left[\hat{k}_1 \dots \gamma_{\lambda_{n-1}}\hat{k}_{n-1}\gamma_{\lambda_{n-1}}\hat{k}_n\gamma_{\lambda_n}\hat{k}_n\hat{p}\hat{k}_n\gamma_{\lambda_n}\hat{k}_{n-1}\gamma_{\lambda_{n-1}} \dots \hat{k}_1\hat{p}\right] . \end{aligned} \tag{3.44}$$

We have used in here the quark density matrix given by eq. (3.11). We are going to calculate $B^{(n)}_q$ in DLA. In order to select appropriate contributions in the trace in eq. (3.44), we generalize the approximation of eq. (3.23) to k_i, with $i = 1, 2, \dots, n-1$:

$$\hat{k}_i\hat{p}\hat{k}_i = 2pk_i\hat{k}_i - k_i^2\hat{p} \approx -k_i^2\hat{p}. \tag{3.45}$$

Doing so we arrive at the DL contribution N^{DL}_q:

$$\begin{aligned} N^{DL}_q &= (-2)^{n-1}k_1^2 \dots k^2_{n-1}(w+2pk_n)\,\mathrm{Tr}[\hat{p}\hat{k}_n\hat{p}\hat{k}_n] \\ &\approx 2^{n-1}k^2_{1\perp} \dots k^2_{n-1\perp}\mathrm{Tr}[\hat{p}\hat{k}_n\hat{p}\hat{k}_n] . \end{aligned} \tag{3.46}$$

Substituting eq. (3.44), we arrive at $B^{(n)}_q$ in DLA. The integration region in DLA was found in ref. [48]:

$$\begin{aligned} &\beta_1 \gg \beta_2 \gg \dots \gg \beta_n , \\ &\frac{k^2_{1\perp}}{\beta_1} \ll \frac{k^2_{2\perp}}{\beta_2} \ll \dots \ll \frac{k^2_{n-2\perp}}{\beta_{n-2}} . \end{aligned} \tag{3.47}$$

Integrations over momenta $k_1, \dots, k_{n-2}$ in the region defined by eq. (3.47) yield DL contributions whereas integration over k_n, k_{n-1} yields the factor $1/x$. Integration over

k_n, k_{n-1} is not restricted by eq. (3.47) but runs over the whole phase space. As is known (see ref. [51]), contributions of non-ladder graphs cancel each other in DLA. Such a straightforward approach is comparatively simple for purely quark ladders (e.g., for the non-singlet structure functions) but becomes too complex for calculating singlets where the quark rungs are mixed with gluon ones. It is more practical to implement evolution equations in this case.

3.5 Remark on contributions of non-ladder graphs

Our analysis of the non-ladder graphs $\sim \alpha_s^2$ shows that they do not yield the factor $1/x$ and because of that they can be neglected. Technically, the reason of their smallness is that they do not contain $(k_2^2)^2$ in denominators. At the same time, non-ladder graphs are essential in higher loops ($\sim \alpha_s^n$, with $n > 2$). They should be accounted for because they bring DL contributions. However, as long as α_s is treated as a constant, DL contributions of the non-ladder graphs cancel each other(see ref. [51]) and therefore they are essential at running α_s only.

4 Calculating B_q and B_g in DLA

We calculate B_q and B_g with constructing and solving IREEs for it. Constructing IREEs in the DIS context was explained in many our papers. For instance, IREEs for the DIS structure function F_1 can be found in [38]; the overview of the technical details can be found in ref. [43]. The essence of this approach is first to introduce a IR cut-off μ to regulate IR divergences of the graphs contributing to $B_{q,g}$ in higher loops.[2] Once such cut-off has been introduced, amplitudes $B_{q,g}$ become μ-dependent and tracing their evolution with respect to μ allows one to construct IREEs. The IREE technology involves the IR cut-off which restricts from below transverse momenta of virtual partons and exploits the fact that DL contributions of the partons with minimal $k_\perp$ can be factorized.

The IREEs for $B_{q,g}$ take a simpler form when the Mellin transform has been used. We are going to calculate dependence of $B_{q,g}$ on both w and Q^2 but the standard parametrization $B_{q,g} = B_{q,g}(x, Q^2/\mu^2)$ leaves the w-dependence to be μ-independent, so as a result we cannot trace it within the IREE technology. Because of that we replace x with the μ-dependent argument w/μ^2, arriving at the parametrization $B_{q,g} = B_{q,g}\left(w/\mu^2, Q^2/\mu^2\right)$. We stress that this replacement is purely technical detail and the standard parametrization will be restored automatically in final expressions for $B_{q,g}$. For the present, we write the Mellin transform for $B_{q,g}$ as follows:

$$B_{q,g}\left(w/\mu^2, Q^2/\mu^2\right) = \int_{-\imath\infty}^{\imath\infty} \frac{d\omega}{2\pi\imath} \left(w/\mu^2\right)^{\omega} f_{q,g}(\omega, Q^2/\mu^2). \tag{4.1}$$

As usually, the integration line in eq. (4.1) runs to the right of the rightmost singularity of $f_{q,g}$. The transform inverse to eq. (4.1) is

$$f_{q,g}(\omega, Q^2/\mu^2) = \int_{\mu^2}^{\infty} \frac{dw}{w} \left(w/\mu^2\right)^{-\omega} B_{q,g}\left(w/\mu^2, Q^2/\mu^2\right) . \tag{4.2}$$

[2]We use the mass scale μ of eq. (1.1) as an IR cut-off for simplicity reason, in order to avoid introducing extra parameters.

Throughout the paper we will address $f_{q,g}$ as Mellin amplitudes. The same form for Mellin transforms we used in ref. [38] for the structure function F_1. It is convenient to use beyond the Born approximation the logarithmic variables ρ defined in eq. (3.18) and y defined as follows:

$$y = \ln\left(Q^2/\mu^2\right). \tag{4.3}$$

IREEs for amplitudes $A_{q,g}$ were obtained in ref. [38] and IREEs for amplitudes $B_{q,g}$ are absolutely the same, so we do not derive them here and only briefly comment on them. IREEs for $B_{q,g}$ in the ω-space look as follows:

$$\begin{aligned} \partial f_q(\omega, y)/\partial y &= \left[-\omega + h_{qq}(\omega)\right] f_q(\omega, y) + f_g(\omega, y) h_{gq}(\omega), \\ \partial f_g(\omega, y)/\partial y &= f_q(\omega, y) h_{qg}(\omega) + \left[-\omega + h_{gg}(\omega)\right] f_g(\omega, y), \end{aligned} \tag{4.4}$$

with $h_{qq}, h_{gq}, h_{qg}, h_{gg}$ being auxiliary amplitudes describing parton-parton scattering in DLA. They can be found in ref. [38]. In addition, explicit expressions for h_{ik} (with $i, k = q, g$) can be found in appendix B. One can see that eqs. (4.4) exhibit a certain similarity to the DGLAP equations. Indeed, the l.h.s. of eqs. (4.4) are the derivatives with respect to $\ln Q^2$. Very soon we will demonstrate that the role of the terms $\sim \omega$ in the r.h.s. of (4.4) is to convert the factor $\left(w/\mu^2\right)^\omega$ into $x^{-\omega}$. The remaining difference between eqs. (4.4) and DGLAP equations is that all anomalous dimensions h_{ik} in eqs. (4.4) are calculated in DLA, i.e. they contain contributions $\sim \alpha_s^{1+n}/\omega^{1+2n}$ to all orders in α_s whereas the DGLAP equations operate with the anomalous dimensions calculated in several fixed orders in α_s. For instance, the most singular terms in the LO DGLAP they are $\sim \alpha_s/\omega$ while NLO DGLAP involves more singular terms. General solution to eq. (4.4) also looks similar to DGLAP expressions:

$$\begin{aligned} f_q(\omega, y) &= e^{-\omega y}\left[C_{(+)} e^{\Omega_{(+)} y} + C_{(-)} e^{\Omega_{(-)} y}\right], \\ f_g(\omega, y) &= e^{-\omega y}\left[C_{(+)} \frac{h_{gg} - h_{qq} + \sqrt{R}}{2h_{qg}} e^{\Omega_{(+)} y} + C_{(-)} \frac{h_{gg} - h_{qq} - \sqrt{R}}{2h_{qg}} e^{\Omega_{(-)} y}\right], \end{aligned} \tag{4.5}$$

This similarity is especially clear as one notices that the overall factor $e^{-\omega y} = \left(\mu^2/Q^2\right)^\omega$ in eq. (4.5) converts the factor $\left(w/\mu^2\right)^\omega$ of eq. (4.1) into the standard DGLAP factor $x^{-\omega}$, when eq. (4.5) is combined with (4.1). The factors $C_{(\pm)}(\omega)$ are arbitrary factors whereas $\Omega_{(\pm)}$ are expressed through h_{ik}:

$$\Omega_{(\pm)} = \frac{1}{2}\left[h_{gg} + h_{qq} \pm \sqrt{R}\right], \tag{4.6}$$

with

$$R = (h_{gg} + h_{qq})^2 - 4(h_{qq}h_{gg} - h_{qg}h_{gq}) = (h_{gg} - h_{qq})^2 + 4h_{qg}h_{gq}\,. \tag{4.7}$$

The next step is to specify coefficient functions $C_{(\pm)}(\omega)$ and we notice that similarity of our approach and DGLAP ends at this point. Indeed, calculating coefficient functions is beyond the scope of DGLAP whereas we continue to apply the IREE approach. Before doing it, let us make use of matching $B_{q,g}$ and amplitudes $\widetilde{B}_{q,g}$ which describe the same process in the kinematics where the external photons are (nearly) on-shell, i.e. with virtualities $Q^2 \approx \mu^2$. It means that $\widetilde{B}_{q,g}$ do not depend on y. It is worth mentioning that our strategy here is to some extent similar to the one of the BFKL-induced models where the BFKL Pomeron is used as an input. In the ω-space the matching is

$$f_q(\omega, y)|_{y=0} = \widetilde{f}_q\,, \qquad f_g(\omega, y)|_{y=0} = \widetilde{f}_g\,, \tag{4.8}$$

where $\widetilde{f}_{q,g}$ are related by the Mellin transform (4.1) to amplitudes $\widetilde{B}_{q,g}$ which describe the same process, however with the external photons being (nearly) on-shell, i.e. with virtualities $Q^2 \approx \mu^2$. It means that $\widetilde{f}_{q,g}$ do not depend on y. Combining eqs. (4.8) and (4.5) lead us to the algebraic system:

$$\begin{aligned} \widetilde{f}_q &= C_{(+)} + C_{(-)}, \\ \widetilde{f}_g &= C_{(+)} \frac{h_{gg} - h_{qq} + \sqrt{R}}{2h_{gq}} + C_{(-)} \frac{h_{gg} - h_{qq} - \sqrt{R}}{2h_{gq}} 2h_{qg}\,, \end{aligned} \tag{4.9}$$

which makes possible to express $C_{(\pm)}$ through $\widetilde{f}_{1,2}$:

$$\begin{aligned} C_{(+)} &= \frac{-\widetilde{f}_q \left(h_{gg} - h_{qq} - \sqrt{R}\right) + \widetilde{f}_g 2h_{qg}}{2\sqrt{R}}\,, \\ C_{(-)} &= \frac{\widetilde{f}_q \left(h_{gg} - h_{qq} + \sqrt{R}\right) - \widetilde{f}_g 2h_{qg}}{2\sqrt{R}}\,. \end{aligned} \tag{4.10}$$

Now we have to calculate $\widetilde{f}_{q,g}$. We do it with constructing and solving appropriate IREEs. These IREEs are

$$\begin{aligned} \omega \widetilde{f}_q(\omega) &= g_q + h_{qq}(\omega)\widetilde{f}_q(\omega) + h_{qg}(\omega))\widetilde{f}_g, \\ \omega \widetilde{f}_g(\omega) &= g_g + h_{gq}(\omega)\widetilde{f}_q(\omega) + h_{gg}(\omega)\widetilde{f}_g(\omega), \end{aligned} \tag{4.11}$$

where inhomogeneous terms $g_{q,g}$ stand for the inputs. We remind that, by definition, the inputs cannot be obtained with evolving some simpler objects. We will specify $g_{q,g}$ in the next section Solution to eq. (4.11) is

$$\begin{aligned} \widetilde{f}_q &= \frac{-g_q(h_{gg} - \omega) + g_g h_{qg}}{\Delta}\,, \\ \widetilde{f}_g &= \frac{g_q a_{gq} - g_q(h_{qq} - \omega)}{\Delta}\,, \end{aligned} \tag{4.12}$$

where

$$\Delta = (\omega - h_{qq})(\omega - h_{qq}) - h_{qg} h_{gq}\,. \tag{4.13}$$

Substituting eq. (4.12) in eq. (4.10) allows us to represent $C_{(\pm)}$ through h_{ik} and inputs $g_{q,g}$. We write $C_{(\pm)}$ in the following form:

$$\begin{aligned} C_{(+)} &= g_q G_q^{(+)} + g_g G_g^{(+)}\,, \\ C_{(-)} &= g_q G_q^{(-)} + g_g G_g^{(-)}\,, \end{aligned} \tag{4.14}$$

JHEP03(2021)274

where

$$
\begin{aligned}
G_q^{(+)} &= \frac{(h_{qg}-\omega)\left(h_{gg}-h_{qq}-\sqrt{R}\right)+2h_{qg}h_{gq}}{2\Delta\sqrt{R}}\,, \\
G_g^{(+)} &= \frac{-h_{gq}\left(h_{gg}-h_{qq}-\sqrt{R}\right)-2h_{qg}(h_{qq}-\omega)}{2\Delta\sqrt{R}}\,, \\
G_q^{(-)} &= \frac{-(h_{qq}-\omega)\left(h_{gg}-h_{qq}+\sqrt{R}\right)-2h_{qg}h_{gq}}{2\Delta\sqrt{R}}\,, \\
G_g^{(-)} &= \frac{h_{gq}\left(h_{gg}-h_{qq}+\sqrt{R}\right)+2h_{qg}(h_{qq}-\omega)}{2\Delta\sqrt{R}}\,.
\end{aligned}
\tag{4.15}
$$

Combining eqs. (4.15), (4.14) and (4.5) leads to expressions for $f_{q,g}$ in terms of h_{ik} and $g_{q,g}$. We remind that explicit expressions for h_{ik} can be found in appendix B. They are known in DLA for both spin-dependent DIS structure function g_1 (see ref. [43]) and for F_1 as well (see ref. [38]). Let us compare eq. (4.11) for $\widetilde{f}_{q,g}(\omega)$ and eq. (4.4) for $f_{q,g}(\omega, y)$. The first difference between them is that eq. (4.11) does not contain the derivative $\partial/\partial y$ because $\widetilde{f}_{q,g}$ do not depend on y. The second difference is the presence of inhomogeneous terms g_q and g_g in eq. (4.11). These terms stand for the inputs, i.e. for the starting point of the evolution. Specifying them is necessary for obtaining explicit expressions for $f_{q,g}$. Below we consider this issue in detail.

5 Specifying inputs g_q and g_g for amplitudes $B_{q,g}$

Specifying inputs g_q and g_g is the key point of our paper because it is here that we deviate from the routine IREE technology. We remind that throughout the history of the IREE approach the inputs have always been defined as the Born contributions whereas contributions of higher loops were obtained with evolving the Born amplitudes. However, this technology cannot apply to calculating amplitudes $B_{q,g}$. Indeed, the Born values for both B_q and B_g are zeros, so substituting them in eq. (4.11) would lead to the system of algebraic homogeneous equations without an unambiguous solution. The next option is to choose the first-loop amplitudes as the inputs. Technically it is possible: they are non-zero (see eq. (2.10)) and evolving them one can obtain $B_{q,g}$ in DLA. However, in this case the important second-loop contributions $B_q^{(2)}$ and $B_g^{(2)}$, each $\sim 1/x$ (see eqs. (3.22), (3.41)), would be left unaccounted because the IR-evolution controls logarithms and cannot generate the factors $1/x$. In section 3.4 we presented the scenario where $B_q^{(2)}$ and $B_g^{(2)}$ were chosen as the inputs and demonstrated that higher loops cannot change this factor. Instead, they can generate DL contributions. Now we implement this scenario in IREEs and choose $B_{q,g}$ as the inputs. To this end, we should express $B_{q,g}^{(2)}$ in the ω-space. In the first place we represent $B_{q,g}^{(2)}$ in the following form:

$$
\begin{aligned}
B_q^{(2)} &= \rho \widetilde{B}_q^{(2)} \\
B_g^{(2)} &= \rho \widetilde{B}_g^{(2)},
\end{aligned}
\tag{5.1}
$$

with $\rho = \ln(w/\mu^2)$ (see eq. (3.17)). Notice that ρ corresponds to $1/\omega^2$ in the ω space (see eq. (4.1)). Then, remembering that the Mellin transform does not affect $1/x$, we write $B_{q,g}^{(2)}$

in the ω-space and obtain the Mellin amplitudes $\varphi_{q,g}$ conjugated to $B^{(2)}_{q,g}$:

$$\varphi_q = \frac{\widetilde{B}^{(2)}_q}{\omega^2} = \left(\frac{\gamma^{(2)} C^{(2)}_q}{x}\right)\frac{1}{\omega^2} \equiv \frac{\gamma^{(2)} b^{(2)}_q(\omega)}{x},$$
$$\varphi_g = \frac{\widetilde{B}^{(2)}_g}{\omega^2} = \left(\frac{\gamma^{(2)} C^{(2)}_g}{x}\right)\frac{1}{\omega^2} \equiv \frac{\gamma^{(2)} b^{(2)}_g(\omega)}{x}. \tag{5.2}$$

Finally, we specify the inputs g_q and g_g of eq. (4.14) as follows:

$$g_q = \varphi_q = \gamma^{(2)} b^{(2)}_q / x,$$
$$g_g = \varphi_g = \gamma^{(2)} b^{(2)}_g / x. \tag{5.3}$$

We remind that choosing these inputs takes us out of the standard form of DLA, where Born amplitudes were considered as the starting point of evolution.

6 Explicit expressions for F_L in DLA

Substituting $g_{q,g}$ of eq. (5.3) in (4.12) and combining the result with eqs. (4.10), (4.5), (4.1), we obtain explicit expressions for $B_{q,g}$. Then, using eq. (2.8) drives us to expressions for $F^{(q,g)}_L$. As the obtained expressions are linear in $g_{q,g}$, we can factorize from them the overall factor $\gamma^{(2)}/x$. To this end we introduce $C'_\pm$:

$$C_\pm = \gamma^{(2)} x^{-1} C'_\pm \; . \tag{6.1}$$

Using eq. (6.1) allows us to represent expressions for $F^{(q,g)}_L$ as follows:

$$F^{(q)}_L = 4\gamma^{(2)} x \int_{-\imath\infty}^{\imath\infty} \frac{d\omega}{2\pi\imath} x^{-\omega}\left[C'_{(+)} e^{\Omega_{(+)} y} + C'_{(-)} e^{\Omega_{(-)} y}\right], \tag{6.2}$$
$$F^{(g)}_L = 4\gamma^{(2)} x \int_{-\imath\infty}^{\imath\infty} \frac{d\omega}{2\pi\imath} x^{-\omega}\left[C'_{(+)} \frac{h_{gg} - h_{qq} + \sqrt{R}}{2h_{qg}} e^{\Omega_{(+)} y} + C'_{(-)} \frac{h_{gg} - h_{qq} - \sqrt{R}}{2h_{qg}} e^{\Omega_{(-)} y}\right].$$

The overall factor $4x$ at eq. (6.2) is the product of the factor $4x^2$ of eq. (2.8) and the factor $1/x$ from the inputs $g_{q,g}$. Eq. (6.2) includes the contributions to $F^{(q,g)}_L$ most essential at small x. It does not include the first-loop contribution and other contributions decreasing at small x (see eq. (2.10)). On the contrary, both $F^{(q)}_L$ and $F^{(g)}_L$ of eq. (6.2) rise when x is decreasing, albeit this does not look obvious. In order to make it seen clearly we consider below the small-x asymptotics of $F^{(q,g)}_L$, which look much simpler than the parent expressions in eq. (6.2).

6.1 Small-x asymptotics of F_L

At $x \to 0$, $F^{(q,g)}_L$ can be approximated by their small-x asymptotics which we denote $(F^{(q,g)}_L)_{AS}$. Technology of calculating the asymptotics is based on the saddle-point method and the whole procedure is identical to the one for F_1. So, we can use the appropriate results of ref. [38]. After the asymptotics of $F_L^{(q,g)}$ have been calculated and convoluted with the parton distributions $\Phi_{q,g}$ (see eq. (2.6)), the small-x asymptotics of F_L is obtained:

$$(F_L)_{AS} \sim \frac{\Pi}{\ln^{1/2}(1/x)} x^{1-\omega_0} \left(Q^2/\mu^2\right)^{\omega_0/2} , \tag{6.3}$$

where the factor Π includes both numerical factors of perturbative origin and values of the quark and gluon distributions in the ω-space at $\omega = \omega_0$. In any form of QCD factorization Π does not contain any dependency on Q^2 or x (see ref. [38] for detail). Then, ω_0 is the Pomeron intercept calculated with DL accuracy. This intercept was first calculated in ref. [38]. We remind that it has nothing in common with the BFKL intercept. It is convenient to represent ω_0 as follows:

$$\omega_0 = 1 + \Delta^{(DL)} . \tag{6.4}$$

Numerical estimates for $\Delta^{(DL)}$ depend on accuracy of calculations. When α_s is assumed to be fixed,[3]

$$\Delta^{(DL)}_{fix} = 0.29 \tag{6.5}$$

and

$$\Delta^{(DL)} = 0.07 \, , \tag{6.6}$$

when the α_s running effects are accounted for. Substituting either eq. (6.5) or eq. (6.6) in eq. (6.3), one easily finds that $F_L \sim x^{-\Delta^{(DL)}}$ at $x \to 0$. The asymptotics of F_1 was calculated in ref. [38] showed that asymptotically $F_1 \sim x^{-\omega_0}$ and therefore $F_L \sim 2xF_1$.

The growth of F_L and xF_1 at small x is caused by the Pomeron behaviour of the parton-parton amplitudes $f_{ik} = 8\pi^2 h_{ik} \sim x^{-\omega_0}$. Amplitudes f_{gg} and f_{gq}, being convoluted with Φ_g and Φ_q, form the gluon distribution in the initial hadron, which we denote G_h:

$$G_h = h_{gg} \otimes \Phi_g + h_{gq} \otimes \Phi_q . \tag{6.7}$$

So, at small x

$$F_L \sim xG_h . \tag{6.8}$$

Another interesting observation following from eq. (6.3) is that

$$2\frac{\partial \ln F_L}{\partial \ln Q^2} + \frac{\partial \ln F_L}{\partial \ln x} \to 1 \tag{6.9}$$

at $x \to 0$. We think that it would be interesting to check this relation with analysis of available experimental data. To conclude discussion of the asymptotics, we notice that the asymptotics as eq. (6.3) should be used within its applicability region, otherwise one should use the expressions of eq. (6.2). The estimate obtained in ref. [38] states that eq. (6.3) can be used at $x \leq 10^{-6}$.

[3]We use here the value $\alpha_s = 0.24$ according to prescription of ref. [47].

JHEP03(2021)274

6.2 Comparison with approaches involving BFKL

Let us start this comparison with considering the second-order graphs (b) and (c) in figure 2, each with a pair of virtual gluons propagating in the t-channel. In section 3 we used the DL configuration, where one of the gluons is longitudinally polarized while polarization of the other gluon is transverse In contrast, contributions to BFKL coming from these graphs involve the kinematics where the both ladder gluons bear longitudinal polarizations. Accounting for these polarizations immediately leads to the following behavior of contributions $B^{(2b)}_{LL}$ and $B^{(2c)}_{LL}$ (the subscripts LL refer to the longitudinal polarizations):

$$B^{(2b)}_{LL} \sim B^{(2c)}_{LL} \sim \frac{1}{x\lambda}, \tag{6.10}$$

with $\lambda = \mu^2/w$. Therefore, $B^{(2b,2c)}_{LL}$ are greater than the considered in section 3 contributions $B^{(2)}_{q,g}$ (we remind that $B^{(2)}_{q,g} \sim 1/x$). Convoluting graphs (b,c) in figure 2 with a hadron and using appropriate hadron impact factors turns the factor λ into x, so the singular factor in eq. (6.10) is now $1/x^2$. This factor cancels the factor x^2 relating $B^{(2b,2c)}_{LL}$ to F_L (see eq. (2.8)). Then, accounting for the impact of higher loops brings the Regge factor $x^{-\Delta_{\mathrm{BFKL}}}$, with Δ_{BFKL} being the intercept of the BFKL Pomeron. Thus we obtain that the BFKL contribution to F_L is

$$F_L \sim x^{-\Delta_{\mathrm{BFKL}}}, \tag{6.11}$$

where Δ_{BFKL} is used in either LO or NLO. In contrast to eq. (6.11), the contribution (6.3) has the extra factor x and because of it (6.11) may look more important than (6.3). However, the leading singularity ω_0 in eq. (6.3) is large, $\omega_0 > 1$ (see eq. (6.4)), so it cancels the factor x and after that $F_L \sim x^{-\Delta_{DL}}$. Thus the small-$x$ behaviour of F_L predicted by eq. (6.3), and the one predicted by eq. (6.11) become very much alike. Indeed, the intercepts of Pomerons in the both approaches are pretty close to each other: $\Delta^{(DL)}_{fix}$ of eq. (6.5) is close to the intercept of the LO BFKL Pomeron and $\Delta^{(DL)}$ of eq. (6.6) practically coincides with the NLO BFKL Pomeron intercept.

On the contrary, the Q^2-dependence predicted by eq. (6.3) differs from predictions given by all other approaches: they do not satisfy eq. (6.9). It means that studying the x-dependence of experimental data for F_L with using Regge fits cannot unambiguously deduce which of these two Pomerons is involved. In order to do it, one should investigate the Q^2-dependence of the data. To conclude this section, we once more stress that these approaches deal with different logarithmic contributions and cannot be related to each other.

6.3 Remark on F_L at arbitrary Q^2

The expressions in eq. (6.2) are valid in the kinematic region (1.1) where Q^2 is large. However, it is easy to generalize eq. (6.2) to small Q^2. It was proved in refs. [38, 43] and used for the structute function F_1 in ref. [52] that such a generalization is achieved with replacement of Q^2 by $Q^2 + \mu^2$. When this shift has been done, $F^{(q)}_L$ and $F^{(q)}_L$ of eq. (6.2) depend on new variables $\bar{x}, \bar{Q}^2$:

$$\bar{Q}^2 = Q^2 + \mu^2, \quad \bar{x} = \bar{Q}^2/w. \tag{6.12}$$

Thus, one can universally use the expressions for $F^{(q,g)}_L$ in eq. (6.2) at arbitrary Q^2 providing the arguments of $F^{(q,g)}_L$ are $\bar{x}$ and $\bar{Q}^2$.

JHEP03(2021)274

7 Conclusions

Our results predict that F_L grows at small x despite the very small factor x^2 at B in eq. (2.5). First, we re-calculated with logarithmic accuracy the available in the literature second-loop contributions $B_q^{(2)}$ and $B_g^{(2)}$, each contains the large power factor $1/x$ in contrast to the Born and first-loop contributions. This calculation allowed us to conclude that $1/x$ will be present in higher-loop expressions and cannot disappear or be replaced by another power factor. We demonstrated that most important contributions coming from higher orders are double logarithms. Accounting for DL contributions to all orders in α_s, we calculated the x and Q^2 -evolution of $B_{q,g}^{(2)}$ in DLA. This evolution proved to be similar to the evolution of the structure function F_1. Eventually we obtained eq. (6.2) for the partonic components $F_L^{(q)}$ and $F_L^{(q)}$ of F_L. The both these components rise at small x though complexity of expressions in eq. (6.2) prevents to see the rise. To make the rise be clearly seen, we calculated the small-x asymptotics of F_L, which proved to be of the Regge type. The asymptotics make obvious that the synergic effect of the factor $1/x$ and the total resummation of double logarithms overcomes smallness of the factor x^2 at B in eq. (2.5) and ensures the rise of F_L at small x, see eq. (6.3). Then in eq. (6.8) we noticed that the rise of F_L and the gluon distributions in the hadrons at small x are identical. We also suggested in eq. (6.9) the simple relation between derivatives of logarithm of F_L. This relation could be checked with analysis of experimental data, so such check could test correctness of our reasoning. The explicit expressions for F_L obtained in section 5 are valid at $Q^2 \geq \mu^2$. In section 6 we obtained the extension of those expressions to the region $Q^2 < \mu^2$. Confronting our results on the asymptotics of F_L with the ones based on BFKL Pomeron, we demonstrated that they predicted the similar small-x behavior and widely different Q^2-dependence.

A Integration in eq. (3.14)

We write eq. (3.14) in the following form:

$$B^{2a} \approx 4C_F^2 \chi_2 \left[I_1^{2a} + I_2^{2a} \right] , \tag{A.1}$$

with $I_{1,2}^{2a}$ defined as integrals over the transverse momenta z_1:

$$\begin{aligned} I_1^{2a} &= \int_\lambda^1 \frac{dz_1}{z_1} J_1^{2a} , \\ I_2^{2a} &= \int_\lambda^1 \frac{dz_1}{z_1} J_2^{2a} , \end{aligned} \tag{A.2}$$

where $J_{1,2}^{2a}$ involve integration over z_2:

$$\begin{aligned} J_1^{2a} &= \int_\lambda^1 dz_2 \frac{z^3}{z_2^2} \widetilde{J}_1^{2a} , \\ I_2^{2a} &= \int_\lambda^1 dz_2 \frac{z^2}{z_2^2} \widetilde{J}_2^{2a} . \end{aligned} \tag{A.3}$$

JHEP03(2021)274

Integrals $\widetilde{J}^{2a}_{1,2}$ deal with integration over the longitudinal variable l:

$$\begin{aligned}
\widetilde{J}^{2a}_1 &= -\int_z^1 \frac{dl}{l^2(l+\eta)^2}\,, \\
\widetilde{J}^{2a}_2 &= \int_z^1 \frac{dl}{l(l+\eta)^2}\,,
\end{aligned} \tag{A.4}$$

with η defined in eq. (3.15). Integration over l in eq. (A.4) yields

$$\begin{aligned}
\widetilde{J}^{2a}_1 &= \frac{1}{\eta^2}\left(1-\frac{1}{z}\right) - \frac{2}{\eta^3}\ln\left(\frac{1+\eta}{z+\eta}\right) + \frac{1}{\eta^3}\left[\frac{1}{1+\eta} - \frac{1}{z+\eta}\right], \\
\widetilde{J}^{2a}_2 &= \frac{1}{\eta^2}\left[-\ln(1+\eta) - \ln\left((z+\eta)/z\right) + \frac{\eta}{1+\eta} - \frac{\eta}{z+\eta}\right]
\end{aligned} \tag{A.5}$$

and therefore

$$\begin{aligned}
J^{2a}_1 &= \int_\lambda^1 dz_2 \left[\frac{z-1}{(z_2+x)^2} - \frac{z_2}{(z_2+x)^3}\ln U(z,z_2)\right. \\
&\left. + \frac{z_2}{(z_2+x)^3}\ln(2z_2+x) + \frac{z_2}{(z_2+x)^3 U(z,z_2)} - \frac{z_2}{(z_2+x)^3(2z_2+x)}\right] \\
J^{2a}_2 &= \int_\lambda^1 dz_2 \frac{1}{(z_2+x)^2}\left[\ln(2z_2+x) - \ln U(z,z_2) - \frac{z_2}{U(z,z_2)} + \frac{z_2}{2z_2+x}\right],
\end{aligned} \tag{A.6}$$

where

$$U(z,z_2) = z_2 + z(z_2+x)\,. \tag{A.7}$$

It is convenient to perform integration in eq. (A.6), using the variable $y = 1/(z_2+x)$ instead of z_2. The most essential contributions in eq. (A.6) at small x are the ones $\sim 1/x$. Accounting for them only, we obtain

$$\begin{aligned}
J^{2a}_1 &= x^{-1}[\ln 2 - 1/2]\,, \\
J^{2a}_2 &= x^{-1}(1/2)\,.
\end{aligned} \tag{A.8}$$

Substituting this result in eq. (A.2), we obtain

$$I^{2a}_1 + I^{2a}_2 = (\rho \ln 2)\; x^{-1}\,. \tag{A.9}$$

B Expressions for h_{ik}

$$\begin{aligned}
h_{qq} &= \frac{1}{2}\left[\omega - Z - \frac{b_{gg}-b_{qq}}{Z}\right], \qquad h_{qg} = \frac{b_{qg}}{Z}\,, \\
h_{gg} &= \frac{1}{2}\left[\omega - Z + \frac{b_{gg}-b_{qq}}{Z}\right], \qquad h_{gq} = \frac{b_{gq}}{Z}\,,
\end{aligned} \tag{B.1}$$

where

$$Z = \frac{1}{\sqrt{2}}\sqrt{Y+W}\,, \tag{B.2}$$

with

$$Y = \omega^2 - 2(b_{qq}+b_{gg}) \tag{B.3}$$

and

$$W = \sqrt{(\omega^2 - 2(b_{qq} + b_{gg}))^2 - 4(b_{qq} - b_{gg})^2 - 16 b_{gq} b_{qg}}\,, \tag{B.4}$$

where the terms $b_{rr'}$ include the Born factors $a_{rr'}$ and contributions of non-ladder graphs $V_{rr'}$:

$$b_{rr'} = a_{rr'} + V_{rr'}\ . \tag{B.5}$$

The Born factors are (see refs. [43, 44] for detail):

$$a_{qq} = \frac{A(\omega) C_F}{2\pi}\,, \qquad a_{qg} = \frac{A'(\omega) C_F}{\pi},\ a_{gq} = -\frac{A'(\omega) n_f}{2\pi}\ . \qquad a_{gg} = \frac{2 N A(\omega)}{\pi}\,, \tag{B.6}$$

where A and A' stand for the running QCD couplings as shown in ref. [47]:

$$A = \frac{1}{b}\left[\frac{\eta}{\eta^2 + \pi^2} - \int_0^\infty \frac{dz e^{-\omega z}}{(z+\eta)^2 + \pi^2}\right], \qquad A' = \frac{1}{b}\left[\frac{1}{\eta} - \int_0^\infty \frac{dz e^{-\omega z}}{(z+\eta)^2}\right], \tag{B.7}$$

with $\eta = \ln\left(\mu^2/\Lambda^2_{QCD}\right)$ and b being the first coefficient of the Gell-Mann- Low function. When the running effects for the QCD coupling are neglected, $A(\omega)$ and $A'(\omega)$ are replaced by α_s. The terms $V_{rr'}$ approximately represent the impact of non-ladder graphs on $h_{rr'}$ (see ref. [43] for detail):

$$V_{rr'} = \frac{m_{rr'}}{\pi^2} D(\omega)\,, \tag{B.8}$$

with

$$m_{qq} = \frac{C_F}{2N}\,, \quad m_{gg} = -2N^2\,, \quad m_{gq} = n_f \frac{N}{2}\,, \quad m_{qg} = -N C_F\,, \tag{B.9}$$

and

$$D(\omega) = \frac{1}{2b^2} \int_0^\infty dz e^{-\omega z} \ln\left((z+\eta)/\eta\right)\left[\frac{z+\eta}{(z+\eta)^2 + \pi^2} - \frac{1}{z+\eta}\right]. \tag{B.10}$$

Let us note that $D = 0$ when the running coupling effects are neglected. It corresponds the total compensation of DL contributions of non-ladder Feynman graphs to scattering amplitudes with the positive signature as was first noticed in ref. [51]. When α_s is running, such compensation is only partial.

Acknowledgments

We are grateful to V. Bertone, N.Ya. Ivanov and Yuri V. Kovchegov for useful communications.

References

[1] E.G. Floratos, D.A. Ross and C.T. Sachrajda, *Higher order effects in asymptotically free gauge theories: the anomalous dimensions of Wilson operators*, Nucl. Phys. B **129** (1977) 66 [*Erratum ibid.* **139** (1978) 545] [INSPIRE].

[2] E.G. Floratos, D.A. Ross and C.T. Sachrajda, *Higher order effects in asymptotically free gauge theories. 2. Flavor singlet Wilson operators and coefficient functions*, Nucl. Phys. B **152** (1979) 493 [INSPIRE].

[3] W.A. Bardeen, A.J. Buras, D.W. Duke and T. Muta, *Deep inelastic scattering beyond the leading order in asymptotically free gauge theories*, Phys. Rev. D **18** (1978) 3998 [INSPIRE].

[4] G. Altarelli, R.K. Ellis and G. Martinelli, *Leptoproduction and Drell-Yan Processes Beyond the Leading Approximation in Chromodynamics*, *Nucl. Phys. B* **143** (1978) 521.

[5] G. Altarelli, R.K. Ellis and G. Martinelli, *Large perturbative corrections to the Drell-Yan process in QCD*, Nucl. Phys. B **157** (1979) 461 [INSPIRE].

[6] G. Altarelli, R.K. Ellis, G. Martinelli and S.-Y. Pi, *Processes involving fragmentation functions beyond the leading order in QCD*, Nucl. Phys. B **160** (1979) 301 [INSPIRE].

[7] J. Kubar-Andre and F.E. Paige, *Gluon corrections to the Drell-Yan model*, Phys. Rev. D **19** (1979) 221 [INSPIRE].

[8] B. Humpert and W.L. Van Neerven, *On the nonleading q anti-q and q g contributions in Drell-Yan processes*, Phys. Lett. B **85** (1979) 293 [INSPIRE].

[9] K. Harada, T. Kaneko and N. Sakai, *Hadronic lepton pair production beyond the leading order in perturbative QCD*, Nucl. Phys. B **155** (1979) 169 [*Erratum ibid.* **165** (1980) 545] [INSPIRE].

[10] R. Baier and K. Fey, *Finite corrections to quark fragmentation functions in perturbative QCD*, Z. Phys. C **2** (1979) 339 [INSPIRE].

[11] G. Curci, W. Furmanski and R. Petronzio, *Evolution of parton densities beyond leading order: the nonsinglet case*, Nucl. Phys. B **175** (1980) 27 [INSPIRE].

[12] W. Furmanski and R. Petronzio, *Lepton-hadron processes beyond leading order in quantum chromodynamics*, Z. Phys. C **11** (1982) 293 [INSPIRE].

[13] A.A. Grigorian, N.Y. Ivanov and A.B. Kaidalov, *Spin in the quark-gluon picture of strong interactions. secondary Regge trajectories*, *Sov. J. Nucl. Phys.* **36** (1982) 867 [*Yad. Fiz.* **36** (1982) 1490] [INSPIRE].

[14] W.L. van Neerven and E.B. Zijlstra, *Order α_S^2 contributions to the deep inelastic Wilson coefficient*, Phys. Lett. B **272** (1991) 127 [INSPIRE].

[15] E.B. Zijlstra and W.L. van Neerven, *Contribution of the second order gluonic Wilson coefficient to the deep inelastic structure function*, Phys. Lett. B **273** (1991) 476 [INSPIRE].

[16] E.B. Zijlstra and W.L. van Neerven, *Order α_S^2 correction to the structure function $F_3(x, Q^2)$ in deep inelastic neutrino-hadron scattering*, Phys. Lett. B **297** (1992) 377 [INSPIRE].

[17] E.B. Zijlstra and W.L. van Neerven, *Order α_S^2 QCD corrections to the deep inelastic proton structure functions F2 and $F(L)$*, Nucl. Phys. B **383** (1992) 525 [INSPIRE].

[18] S. Moch and J.A.M. Vermaseren, *Deep inelastic structure functions at two loops*, Nucl. Phys. B **573** (2000) 853 [hep-ph/9912355] [INSPIRE].

JHEP03(2021)274

[19] D.I. Kazakov, A.V. Kotikov, G. Parente, O.A. Sampayo and J. Sanchez Guillen, *Complete quartic* (α_s^2) *correction to the deep inelastic longitudinal structure function $F(L)$ in QCD*, *Phys. Rev. Lett.* **65** (1990) 1535 [*Erratum ibid.* **65** (1990) 2921] [INSPIRE].

[20] S. Moch, J.A.M. Vermaseren and A. Vogt, *The longitudinal structure function at the third order*, *Phys. Lett. B* **606** (2005) 123 [hep-ph/0411112] [INSPIRE].

[21] G. Altarelli and G. Parisi, *Asymptotic Freedom in Parton Language*, *Nucl. Phys. B* **126** (1977) 297.

[22] V.N. Gribov and L.N. Lipatov, *Deep inelastic ep scattering in perturbation theory*, *Sov. J. Nucl. Phys.* **15** (1972) 438 [*Yad. Fiz.* **15** (1972) 781] [INSPIRE].

[23] L.N. Lipatov, *The parton model and perturbation theory*, *Yad. Fiz.* **20** (1974) 181 [*Yad. Fiz.* **20** (1974) 181] [INSPIRE].

[24] Y.L. Dokshitzer, *Calculation of the structure functions for deep inelastic scattering and e^+e^- annihilation by perturbation theory in quantum chromodynamics*, *Sov. Phys. JETP* **46** (1977) 641 [*Zh. Eksp. Teor. Fiz.* **73** (1977) 1216] [INSPIRE].

[25] E.A. Kuraev, L.N. Lipatov and V.S. Fadin, *Multi-Reggeon processes in the Yang-Mills theory*, *Sov. Phys. JETP* **44** (1976) 443 [*Zh. Eksp. Teor. Fiz.* **71** (1976) 840] [INSPIRE].

[26] E.A. Kuraev, L.N. Lipatov and V.S. Fadin, *The Pomeranchuk singularity in nonabelian gauge theories*, *Sov. Phys. JETP* **45** (1977) 199 [*Zh. Eksp. Teor. Fiz.* **72** (1977) 377] [INSPIRE].

[27] I.I. Balitsky and L.N. Lipatov, *The Pomeranchuk Singularity in Quantum Chromodynamics*, *Sov. J. Nucl. Phys.* **28** (1978) 822 [*Yad. Fiz.* **28** (1978) 1597] [INSPIRE].

[28] V.S. Fadin and L.N. Lipatov, *BFKL Pomeron in the next-to-leading approximation*, *Phys. Lett. B* **429** (1998) 127 [hep-ph/9802290] [INSPIRE].

[29] M. Ciafaloni and G. Camici, *Energy scale(s) and next-to-leading BFKL equation*, *Phys. Lett. B* **430** (1998) 349 [hep-ph/9803389] [INSPIRE].

[30] J. Kwiecinski, A.D. Martin and A.M. Stasto, *A unified BFKL and GLAP description of F2 data*, *Phys. Rev. D* **56** (1997) 3991 [hep-ph/9703445] [INSPIRE].

[31] R.D. Ball, V. Bertone, M. Bonvini, S. Marzani, J. Rojo and L. Rottoli, *Parton distributions with small-x resummation: evidence for BFKL dynamics in HERA data*, *Eur. Phys. J. C* **78** (2018) 321 [arXiv:1710.05935] [INSPIRE].

[32] G. Altarelli, R.D. Ball and S. Forte, *Resummation of singlet parton evolution at small x*, *Nucl. Phys. B* **575** (2000) 313 [hep-ph/9911273] [INSPIRE].

[33] G. Altarelli, R.D. Ball and S. Forte, *Small x resummation and HERA structure function data*, *Nucl. Phys. B* **599** (2001) 383 [hep-ph/0011270] [INSPIRE].

[34] Y.V. Kovchegov, *Small x $F(2)$ structure function of a nucleus including multiple Pomeron exchanges*, *Phys. Rev. D* **60** (1999) 034008 [hep-ph/9901281] [INSPIRE].

[35] A. Luszczak and H. Kowalski, *Dipole model analysis of highest precision HERA data, including very low Q^2's*, *Phys. Rev. D* **95** (2017) 014030 [arXiv:1611.10100].

[36] J.L. Albacete, N. Armesto, J.G. Milhano, P. Quiroga-Arias and C.A. Salgado, *AAMQS: a non-linear QCD analysis of new HERA data at small-x including heavy quarks*, *Eur. Phys. J. C* **71** (2011) 1705 [arXiv:1012.4408] [INSPIRE].

[37] xFitter Developers' Team collaboration, *Impact of low-x resummation on QCD analysis of HERA data*, *Eur. Phys. J. C* **78** (2018) 621 [arXiv:1802.00064] [INSPIRE].

[38] B.I. Ermolaev and S.I. Troyan, *Singlet structure function F_1 in double-logarithmic approximation*, *Eur. Phys. J. C* **78** (2018) 204 [INSPIRE].

[39] L.N. Lipatov, *Multi-Regge processes in gravitation*, *Sov. Phys. JETP* **55** (1982) 582 [*Zh. Eksp. Teor. Fiz.* **82** (1982) 991] [INSPIRE].

[40] L.N. Lipatov, *Graviton reggeization*, *Phys. Lett. B* **116** (1982) 411 [INSPIRE].

[41] R. Kirschner and L.N. Lipatov, *Doubly logarithmic asymptotic of the quark scattering amplitude with nonvacuum exchange in the T channel*, *Zh. Eksp. Teor. Fiz.P* **83** (1982) 488.

[42] R. Kirschner and L.n. Lipatov, *Double logarithmic asymptotics and Regge singularities of quark amplitudes with flavor exchange*, *Nucl. Phys. B* **213** (1983) 122 [INSPIRE].

[43] B.I. Ermolaev, M. Greco and S.I. Troyan, *Overview of the spin structure function g1 at arbitrary x and Q2*, *Riv. Nuovo Cim.* **33** (2010) 57.

[44] B.I. Ermolaev, M. Greco and S.I. Troyan, *Infrared evolution equations: method and applications*, *Acta Phys. Polon. B* **38** (2007) 2243 [arXiv:0704.0341] [INSPIRE].

[45] P.M. Stevenson, *Optimized perturbation theory*, *Phys. Rev. D* **23** (1981) 2916 [INSPIRE].

[46] V.V. Sudakov, *Vertex parts at very high-energies in quantum electrodynamics*, *Sov. Phys. JETP* **3** (1956) 65 [*Zh. Eksp. Teor. Fiz.* **30** (1956) 87] [INSPIRE].

[47] B.I. Ermolaev and S.I. Troyan, *Parametrization of the QCD coupling in the evolution equations*, *Phys. Lett. B* **666** (2008) 256 [arXiv:0805.2278] [INSPIRE].

[48] V.G. Gorshkov, V.N. Gribov, L.N. Lipatov and G.V. Frolov, *Doubly logarithmic asymptotic behavior in quantum electrodynamics*, *Yad. Fiz.* **6** (1967) 129 [*Yad. Fiz.* **6** (1967) 129] [INSPIRE].

[49] V.G. Gorshkov, V.N. Gribov, L.N. Lipatov and G.V. Frolov, *Backward electron-positron scattering at high-energies*, *Yad. Fiz.* **6** (1967) 361 [*Yad. Fiz.* **6** (1967) 361] [INSPIRE].

[50] V.G. Gorshkov, *Electrodynamical processes in opposed high-energy particle beams*, *Usp. Fiz. Nauk.* **110** (1973) 45.

[51] V.G. Gorshkov, L.N. Lipatov and M.M. Nesterov, *On j-plane singularities of e-minus muon-minus scattering amplitudes*, *Yad. Fiz.* **9** (1969) 1221 [INSPIRE].

[52] B.I. Ermolaev, S.I. Troyan, *Combining the small-x evolution and DGLAP for description of inclusive photon induced processes*, *Eur. Phys. J. C* **80** (2020) 98.

JHEP03(2021)274